IEEE Access
Multidisciplinary | Rapid Review | Open Access Journal

Received May 7, 2020, accepted May 23, 2020, date of publication May 28, 2020, date of current version June 22, 2020.

Digital Object Identifier 10.1109/ACCESS.2020.2998373

Effects of Environmental Factors on Partial Discharge Activity and Estimation of Insulation Lifetime in Electrical Machines

WAQAR HASSAN[1], GHULAM AMJAD HUSSAIN[2], (Senior Member, IEEE), FARHAN MAHMOOD[1], SALMAN AMIN[3], AND MATTI LEHTONEN[4], (Member, IEEE)

[1]Department of Electrical Engineering, University of Engineering and Technology (UET) Lahore, Lahore 54890, Pakistan
[2]Department of Engineering, College of Engineering and Applied Sciences, American University of Kuwait (AUK), Safat 13034, Kuwait
[3]Department of Electrical Engineering, University of Engineering and Technology Taxila, Taxila 47050, Pakistan
[4]Department of Electrical Engineering and Automation, School of Electrical Engineering, Aalto University, 02150 Espoo, Finland

Corresponding author: Ghulam Amjad Hussain (ghussain@auk.edu.kw)

This work was supported by the Kuwait Foundation for the Advancement of Sciences (KFAS) under Project PR18-18EO-01.

ABSTRACT Partial discharges (PD) are produced in the stator insulation of electrical machines while energized. The sources of PD are internal voids, crack, and manufacturing defects, which keep on extending with its normal operation, leading to the complete failure of insulation. The intensity of PD is considerably influenced by the environmental factors, including surrounding temperature, pressure, humidity, and contamination. This paper investigates the influence of these factors on the PD activity in electrical machines and estimates the lifetime of insulation. The PD measurements were conducted by placing the motors in a climate-controlled chamber. The PD trend under varying environmental stresses was investigated over time. Accordingly, PD inception voltage and various discharge characteristic parameters such as accumulated apparent charge, cumulative energy function, average discharge current, discharge power, and quadratic rate have been determined. The combined effect of various environmental stresses on the PD activity was also investigated. The mathematical relationships were developed to estimate the discharge characteristics as the functions of pressure and temperature using the Gaussian model and the Exponential model. Finally, the endurance of insulation was estimated under different environmental conditions based on the average discharge current to differentiate between correct and incorrect PD measurements and to develop a right maintenance schedule for motors in service.

INDEX TERMS Environmental stress, lifetime assessment, low voltage motors, insulation, partial discharge.

I. INTRODUCTION

Electric motor is the backbone of the process industry. The reliable operation and lifetime of any motor depend upon its insulation health and conductivity of the winding [1]–[3]. Under normal operation, the partial discharges (PD) are produced in the motor due to voids, cracks and other manufacturing defects in the insulating material [4]–[7]. It has been observed that PD activity is not only dependent on its operating characteristics such as operating voltage, load ratio and speed ratio [8], but also considerably affected by variable environmental conditions. The endurance and the lifetime of the insulation can be correctly estimated by carrying out the PD measurements at actual pressure (p), temperature (T), relative humidity (RH), and contamination in the surrounding environment of an operating machine. Therefore, the PD measurements conducted under the conditions far from the actual environmental conditions can either underestimates or overestimates the life of insulation and makes the maintenance scheduling less certain.

Several studies have been conducted by the researchers to investigate the effect of individual environmental parameters on the PD characteristics of high voltage (HV) insulation [9]–[13]. The impact of seasonal variation on PD activity in rotating machines was reported in [14]. The effect of humidity and temperature on PD measurements in stator winding was presented in [15], [16]. The impact of high temperature on PD activity and the insulation degradation

The associate editor coordinating the review of this manuscript and approving it for publication was Qinfen Lu.

was studied in [17]–[19]. The correlation between discharge magnitude and the temperature was presented in [20], [21]. In [22], the authors employed the dissipated discharge energy to predict the life of insulation under variable pressure, temperature, and humidity conditions. The phase-resolved partial discharge (PRPD) pattern was employed in [23] to specify the condition of stator insulation.

Previous studies have mainly presented the PD characteristics of insulation by considering the impact of pressure, temperature, and humidity individually. As a matter of fact, considerable variability exists in PD characteristics and the insulation lifetime when more than one environmental factors are taken into consideration. On the other hand, contamination is very common due to leakage of various gases and available solid particles in the surrounding in the process industry [24]. Therefore, additional work is required to investigate the effect of contamination on PD characteristics. Thus, the main contribution of this work is to further investigate the combined effect of pressure, temperature, humidity, and contamination on the PD characteristics and the insulation lifetime. To the best of our knowledge, none of the existing literature investigated the impact of contamination on the low voltage insulation of electrical motors at various humidity levels. Furthermore, the development of mathematical models to quantify the PD characteristics under variable environmental conditions is required to ensure the correct PD measurements.

In this paper, the effects of pressure, temperature, humidity, and contamination on PD measurements in low voltage electrical machines were investigated through offline PD testing in a climate-controlled chamber. The environmental stresses were individually applied to investigate their impact on the PD inception voltage (U_i), accumulated apparent charge (q_a), cumulative energy (CE), average discharge current (I), discharge power (P), and quadratic rate (D). The combined effect of temperature, humidity, and contamination on PD activity have been also evaluated in this work. In addition, the mathematical models that characterized the relationships between the environmental conditions and the discharge characteristics were developed. Finally, the insulation lifetime was estimated under different environmental conditions based on the average discharge current.

The rest of the paper is organized as follows: Section II presents the PD phenomenon and the electrical mechanism of PD activity. In Section III, the measurement set-up including the construction of climate-controlled chamber, circuit diagram, PD measurement procedure and the assessment of discharge characteristics is detailed. Section IV presents the measurement results and discussions related to the effect of various environmental factors on PD activity. In section V, the estimation of the insulation lifetime is carried out under different environmental conditions. Finally, in section VI, conclusions are drawn.

II. PARTIAL DISCHARGE PHENOMENON

The PD is defined as a localized electrical discharge that only partially bridges the insulation between electrodes and which may or may not occur adjacent to a conductor. Mostly, PD appears as current or voltage pulses having a very small duration [23]. These pulses are highly dependent on the applied voltage, nature of dielectric material and the environmental conditions. The main causes of PD are the voids, cracks, surface contamination and irregularities in the solid insulation during manufacturing [25]. PD can be classified into surface discharge, internal (cavity and treeing) discharge, and the corona discharge. The surface discharges are produced on the surface of the insulation where the tangential field is high. These discharges are less dangerous than the internal discharges and may be tolerated for a longer duration. The discharges from the void, foreign particle, and cracks in solid insulation are known as internal or cavity discharges. The ionization of the gas surrounding an electrode or bare conductor occurs, when the electric field around the surface of an electrode exceeds the breakdown limit of the gas molecules. This is known as corona discharge [26], [27].

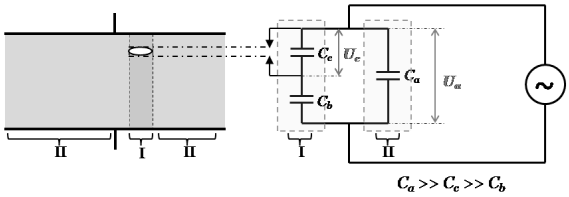

FIGURE 1. Equivalent circuit of a dielectric with cavity.

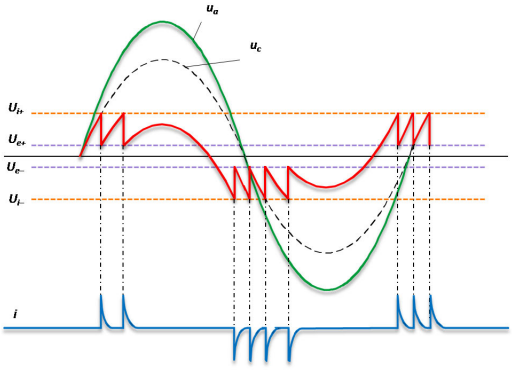

FIGURE 2. Electrical mechanism of PD activity.

A. ELECTRICAL MECHANISM OF PD ACTIVITY

The electrical characteristics of a PD activity can be explained with respect to the well-known three capacitance model, given in Fig. 1 [25]–[27]. Fig. 1 shows the three capacitances C_c, C_b and C_a representing capacitance of the cavity, a capacitance of healthy insulation in series with cavity and healthy insulation in parallel with a series combination of C_c and C_b respectively. The applied voltage U_a and the voltage drop across the cavity U_c are related by (1).

$$U_c = \left(\frac{C_b}{C_c + C_b}\right)U_a \tag{1}$$

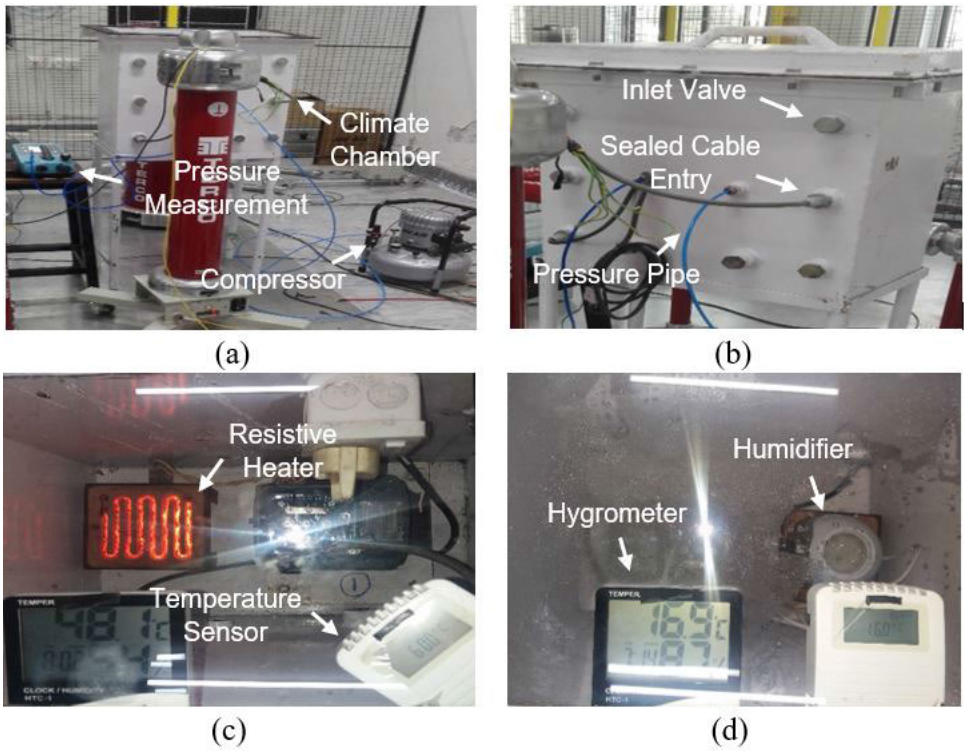

FIGURE 3. Different views of internal (through a glass window) and external arrangements of the climate-controlled chamber.

The sinusoidal variation in the applied voltage $U_a = U_p sin(\omega t + \phi)$ throughout its complete cycle is shown in Fig. 2. The increase in the U_a increases the cavity voltage U_c. When U_c increase to such a value that it approaches the breakdown voltage U_{i+} (in the positive half cycle), the cavity collapses and rapid displacement of charge takes place inside the cavity. This charge is known as space charge. The transformation of charge drops the potential difference across the cavity to a value U_{e+} (extinction voltage, in the positive half cycle) at which the electric field intensity becomes lower than that of the required level to maintain the discharge. At this moment, the discharge ceases and the accumulation of charge starts across the boundaries of the cavity. Due to an increase in the U_a, U_c starts to build-up. Again, when the PD collapses at the U_{i+}, another PD event takes place. Thus, the PD activity goes on repeatedly during both positive and negative cycles of the applied voltage [26], [28]. $U_{i+/-}$ is also called PD inception voltage, represented by U_i.

III. PD MEASUREMENT SET-UP

This research work was carried out by simulating the variable environmental conditions in the laboratory. A series of experiments were conducted to study the effects of environmental stresses on PD measurements.

A. CONSTRUCTION OF CLIMATE-CONTROLLED CHAMBER

The climate-controlled chamber was made out of a 3 mm thick mild steel sheet with removable top plate and gasket seal, having dimensions 90 cm - 76 cm - 76 cm. A 10-10 cm hardened glass window was fixed at the top side for visual inspection during the experiment. The thermally and electrically insulated epoxy was applied at the inner and outer sides of the chamber. The internal and external arrangements of the climate chamber are shown in Fig. 3. The chamber was equipped with an electric heater, humidifier and air circulation fan to ensure constant temperature and humidity throughout the chamber. The temperature inside the chamber was varied from 30° C to 160° C and humidity was varied from 50% to 97%. A compressor and a vacuum pump were attached to the chamber to facilitate the variation of the absolute pressure from 150 mbar to 1800 mbar. A removable dead plug was fixed on the sides to attach the blower pipe to inject contaminants into the chamber. The attached instruments were electronically controlled to achieve the maximum accuracy of the measurements. The p, T, and RH were measured with digital electronic meters.

B. LAYOUT AND CIRCUIT DIAGRAM

The schematic diagram of the PD measurement system is shown in Fig. 4. The PD set-up comprises of the voltage regulator (T_1), PD free step-up transformer (T_2) having PD magnitude less than 5 pC, protective resistor (R_1) of 2.5 MΩ, a coupling capacitor (C) of 10 nF, a quadrupole which converts PD current pulse to a voltage signal, a PD meter and the test object (M) which is an electric motor. One phase of the motor was connected to C and the remaining two

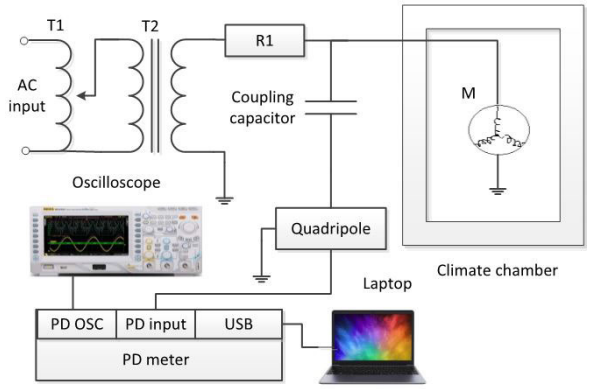

FIGURE 4. Schematic diagram of the PD measuring system used to study the impact of environmental stresses on the insulation used in low voltage motors.

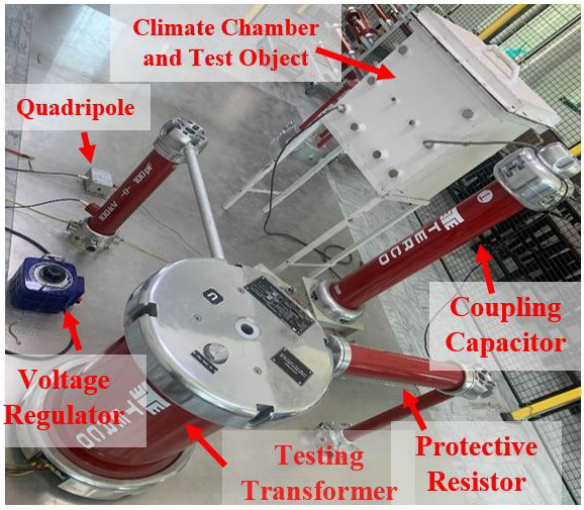

FIGURE 5. PD measurement set-up established in the laboratory.

phases were grounded for safety. The PD meter consisted of a measurement and analysis system with a digital oscilloscope having analog bandwidth of 50 MHz, the input impedance of 50 Ω and a sampling rate of 500 MS/s [29].

The basic noise level (BNL) of less than 0.2 pC and linearity error of less than 0.1 dB was achieved using a broadband filter. The connections of M with the measuring circuit were made using shielded cables with a maximum length of 1 meter. Four motors from two different manufacturers were selected for the experimental work, i.e.

1) Motor-1: 18 kW, 400 V, 50 Hz, make: ABB
2) Motor-2: 18 kW, 400 V, 50 Hz, make: COMER

The physical locations of various components described above are shown in Fig. 5. The calibration of the PD measurement system with the applied circuit topology was carried out according to IEC standard [23] to ensure precise measurements. For this purpose, the voltage supply was detached and a pulse generator (calibrator) was attached in parallel across the test object. A known magnitude of charge (5 pC, 50 pC, 500 pC or 5000 pC) was injected into the test circuit.

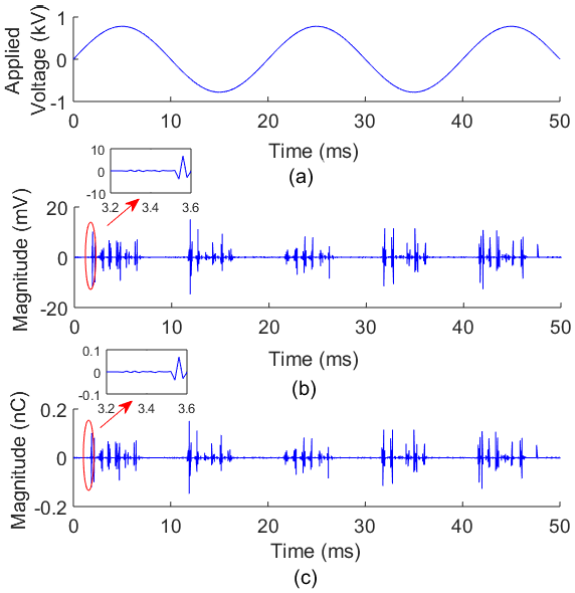

FIGURE 6. Typical PD measurements (a) applied voltage, (b) Magnitude of PD pulses (mV), and (c) PD apparent charge (nC).

The measured charge from the PD meter was then scaled/corrected according to the known injected charge through the calibrator. This was achieved using the correction adjustment knob until the magnitude of charge at PD meter was the same as the magnitude of charge injected through the calibrator. With every change in the test object, the calibration was repeated to ensure accuracy in the PD measurements.

C. MEASUREMENT PROCEDURE AND ASSESSMENT OF PD CHARACTERISTICS

When a constant test voltage is applied to the motor, PD inception voltage varies with environmental conditions, and the corresponding change in electrical stresses conceal the effect of environmental stresses on PD activity. To overcome this problem, the test voltage was raised slowly to measure the PD inception voltage and the PD characteristics were studied at variable voltages ranging up to $1.5 \times U_i$. By varying test voltage (U_a) to $1.5 \times U_i$, the ratio of (U_a/U_i) was kept constant, which nullifies the effect of overvoltage on the PD activity. In this way, the insulation will be subjected to only environmental stresses. A typical measurement of PD activity upon applying $1.5 \times U_i$ is shown in Fig. 6. Fig. 6(a) shows the applied voltage $U_a(t_i)$, Fig. 6(b) is the measured PD signal showing the amplitudes of PD pulses in mV $U_{pd}(t_i)$ and Fig. 6(c) represents the converted PD amplitude into pC, using (2)

$$q_i = C \times U_{pd}(t_i) \tag{2}$$

where C is the coupling capacitance and t_i is the sampling instant.

The PD characteristics can be assessed using several parameters related to the PD signal (i.e. U_i, q_a, CE, I, P and D), which provide the condition of the stator insulation.

Therefore, the PD characteristic parameters can be used to investigate the effect of environmental stresses on the stator winding insulation [23].

1) PD INCEPTION VOLTAGE

The PD inception voltage (U_i) is the applied voltage at which repetitive partial discharges are first observed in the test object, when the voltage applied to the object is gradually increased from a lower value at which no partial discharges are observed. In practice, it is the lowest test voltage at which the magnitude of discharge quantity becomes equal to, or exceeds a specific low value [23]. The PD activity under variable environmental stresses was studied by determining its respective U_i. The test was repeated 5 times at every specific environmental condition, and the average values of U_i were calculated.

2) ACCUMULATED APPARENT CHARGE

Accumulated apparent charge (q_a) is the sum of the individual apparent charge q_i of all the pulses exceeding a specified threshold level during a chosen time frame T_{ref} [23]. It is calculated by (3)

$$q_a = \sum_{i=1}^{N} q_i \tag{3}$$

where q_i is the single sample apparent charge, measured by the digitizer/ oscilloscope and N is the total number of samples in a signal. A typical q_i signal is shown in Fig. 6(c). T_{ref} in all the measurements was selected as 50 ms.

3) CUMULATIVE ENERGY FUNCTION

The CE, up to the total signal duration t_N, across the fixed measuring resistance (R) of the oscilloscope, were determined using (4) [30]–[32]

$$CE = \frac{\Delta t}{R} \sum_{i=1}^{N} (U(t_i))^2 \tag{4}$$

where Δt is the sampling duration or the time difference between two consecutive samples, and $U(t_i)$ is the PD sample voltage at its sampling time instant t_i, as shown in Fig. 6(b).

4) AVERAGE DISCHARGE CURRENT

The average discharge current (I) is a derived quantity and the sum of the absolute values of individual apparent charge magnitudes q_i during a chosen reference time interval T_{ref}, as shown in 6(c), divided by this time interval. It is given in (5).

$$I = \frac{1}{T_{ref}} \times (|q_1| + |q_2| + \ldots\ldots\ldots + |q_i|) \tag{5}$$

5) DISCHARGE POWER

The discharge power (P) is the average power of a PD signal during T_{ref}, as shown in (6) [23].

$$P = \frac{1}{T_{ref}} \times (q_1 U_1 + q_2 U_2 + \ldots\ldots\ldots + q_i U_i) \tag{6}$$

where $U_1, U_2, \ldots U_i$ are the values of the instantaneous test voltage (given by Fig. 6(a)) at the time of occurrence of q_i (given by Fig. 6(c)).

6) QUADRATIC RATE

The quadratic rate (D) is determined from the sum of the square of q_i during T_{ref}, divided by this time interval, as given in (7).

$$D = \frac{1}{T_{ref}} \times (q_1^2 + q_2^2 + \ldots\ldots\ldots + q_i^2) \tag{7}$$

IV. RESULTS AND DISCUSSION

A. EFFECT OF PRESSURE ON PD ACTIVITY

Electric motors are used in aircrafts where the pressure may reach down to 116 mbar [33]. Furthermore, high-pressure vestibules are mostly used for the separation of different atmospheric conditions and act as an air curtain. The air inside these pressure boundaries is above the atmospheric pressure. Electric motors, compressors, and ventilation fans are used in these applications. Therefore, the impact of both positive and negative pressures on the winding wire insulation is required to be investigated because it plays an important role in estimating the lifetime of the motor. The PD measurements were carried out both in the positive and negative pressure ranges from 180 mbar to 1750 mbar at ambient temperature and humidity. The results are shown in Fig. 7. It was observed that the PD activity decreased by increasing p from 180 mbar to 1000 mbar (atmospheric pressure) and further up to 1350 mbar. The minimum discharge magnitude was observed at 1350 mbar. The magnitude of the PD characteristic parameters increased by further increasing p up to 1750 mbar.

The PD measurements at different pressure levels are shown in Fig. 8. It was observed that both the PD magnitude and the number of pulses per cycle increased by changing the atmospheric pressure in any direction (positive or negative pressures). More severity was observed in PD magnitude by increasing the pressure in the negative side than in the positive side.

At low pressures, enhanced PD activity is likely due to the reduced relative air density. The decrease in the relative air density increases the electron mean free path (λ) as given in (8) and (9) [17], [22].

$$\lambda = \frac{\lambda_o}{\delta} \tag{8}$$

$$\delta = \frac{p}{R \times T} \tag{9}$$

where δ is the air density for dry air, P is the pressure, R is specific air constant and T is the temperature. Consequently, the electrons carry more energy and generate electric discharges by crossing more distance between two collisions. When pressure is increased, the PD activity is reduced due to the increased relative air density and associated mean free path is reduced which provides smaller energy to the PD electrons. At high pressures, more PD electrons gain energy

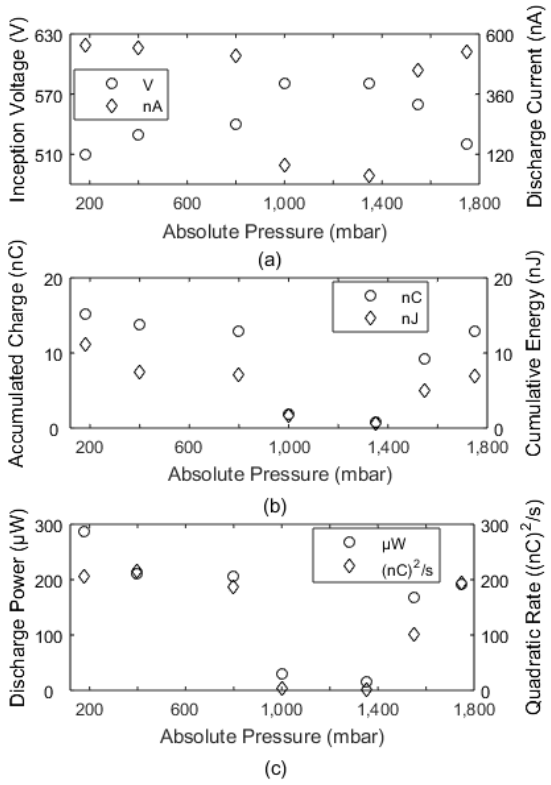

FIGURE 7. PD characteristics measured for different pressures at ambient temperature (35° C) and 58% *RH* (a) inception voltage and average discharge current, (b) accumulated apparent charge and cumulative energy, (c) discharge power and quadratic rate.

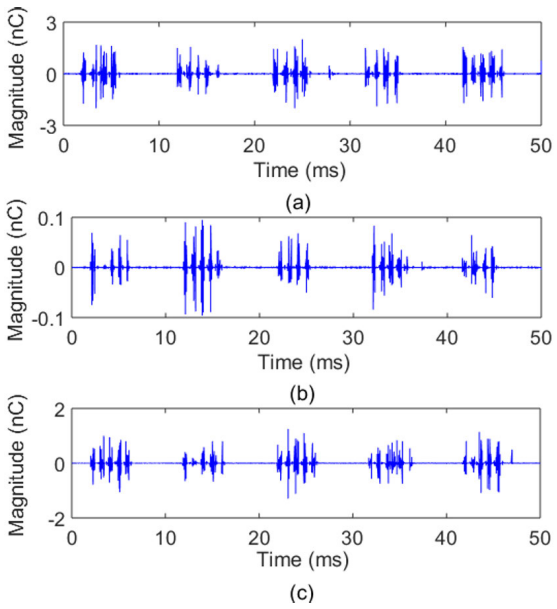

FIGURE 8. PD measurements at different pressures (a) 180 mbar, (b)1000 mbar, and (c) 1750 mbar at ambient temperature (35° C) and 58% *RH*.

but each electron, moving along a shorter distance between two collisions, gains less energy. Therefore, less is the gain of energy and less is dissipated into thermal diffusion, and more energy is injected into the discharge processes [34]. Therefore, more energy will be confined in the discharges at high pressures.

The variations in CE, q_a and I were found as functions of p at ambient temperature and humidity. From experimental results, it was observed that the significant change in the p from the atmospheric pressure (p_{atm}) to either positive or negative direction increased the PD activity. The gauge pressure (p_g) was measured from the absolute pressure (p) and the atmospheric pressure (p_{atm}) using (10).

$$p_g = p - p_{atm} \tag{10}$$

The various models i.e. Gaussian, Exponential and Polynomial equations were developed though curve fitting to establish the relationship between the PD characteristic parameters and the pressure. The R-square goodness of fit hypothesis was applied to measure the closeness of data with the fitted line. Based on the results of R-square goodness of fit hypothesis, the plausibility of two terms Gaussian model was established.

The correlation between CE and p_g is shown in (11).

$$CE = 11.28e^{-(\frac{p_g+1037}{879.8})^2} + 30.79e^{-(\frac{p_g-655.5}{76.52})^2} \tag{11}$$

The Gaussian models developed for q_a and I as functions of p_g at ambient temperature and humidity are represented by (12) and (13), respectively.

$$q_a = 15.78e^{-(\frac{p_g+624.5}{576.6})^2} + 47.88e^{-(\frac{p_g-656.2}{81.87})^2} \tag{12}$$

$$I = 619.6e^{-(\frac{p_g+580.8}{546.9})^2} + 1014e^{-(\frac{p_g-565.01}{116.9})^2} \tag{13}$$

B. EFFECT OF TEMPERATURE ON PD ACTIVITY

The impact of thermal stresses on the winding insulation of low voltage motor was investigated. The measurements of PD characteristic parameters with T at ambient p and humidity are shown in Fig. 9. By increasing the temperature from 35° C to 160° C, U_i decreased from 580 V to 500 V, q_a increased from 1.826 nC to 14.95 nC, and CE increased from 1.606 nJ to 10.995 nJ.

Fig. 10 indicates that PD behavior under thermal stress at ambient pressure is quite different from the PD behavior observed under varying pressure levels. The PD magnitude increased by increasing the temperature but the number of PD pulses per cycle decreased. In LV motors, only weaker points in insulation are significantly affected by increasing the temperature, resulting in high magnitude of PD pulses. The effect of temperature is relatively less when the insulation is in better condition.

The dependence of PD characteristic parameters on temperature can be explained in two ways. Firstly, when T in the chamber is increased, the PD electrons gain thermal energy. Additionally, as with the lower pressure, the relative air density decreases at high temperature. The decrease in the relative air density increases the electron mean free path. Consequently, the electrons gain more energy and generate electric discharges by crossing more distance between two collisions. Secondly, an increase in the equilibrium temperature of the insulation material reduces the additional energy

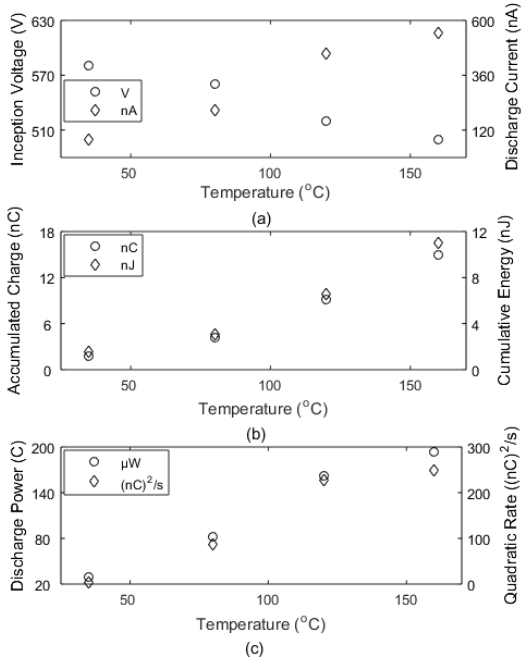

FIGURE 9. PD characteristics measured for different temperatures at ambient pressure (1000 mbar) and 58% *RH* (a) inception voltage and average discharge current, (b) accumulated apparent charge and cumulative energy, (c) discharge power and quadratic rate.

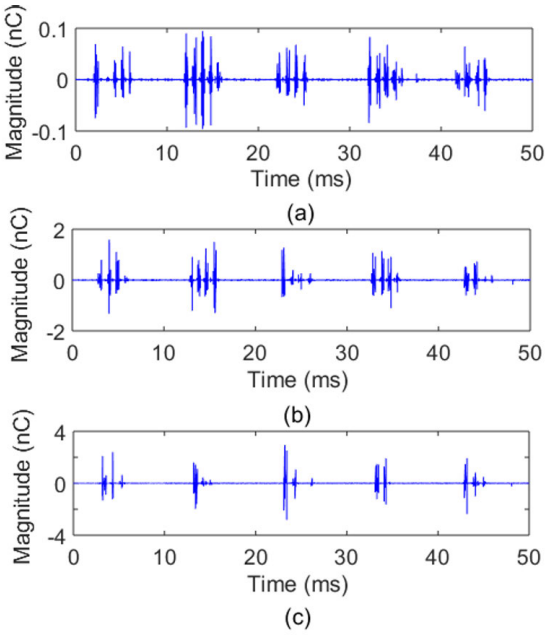

FIGURE 10. PD measurements at different temperatures (a) 35° C, (b) 80° C, and (c) 160° C at ambient pressure (1000 mbar) and humidity (58%).

required from bombarding electrons [17]. Therefore, the discharges are more active and harmful at high temperatures resulting in the faster degradation of the insulation material.

The correlations between various PD characteristic parameters as a function of T at ambient p and humidity were obtained through curve fitting. The validity of the

TABLE 1. The coefficient of variance (β) calculated before and after the moderation.

Variables	CE	q_a	I
p_g	0.252	0.159	0.331
T	0.845	0.757	0.764
p_gT	0.967	0.849	0.783

Exponential models developed for both CE and q_a was established, based on the R-square goodness of fit hypothesis. The exponential equations for CE and q_a as functions of T are given in (14) and (15), respectively.

$$CE = 0.772e^{0.0178T} - 2.531e^{0.23T-16} \tag{14}$$

$$q_a = 0.9e^{0.01924T} - 3.963e^{0.23T-16} \tag{15}$$

The single term Gaussian model developed between I and T provide strong relationship, that was validated based on R-square goodness of fit hypothesis. The correlation between I and T is represented by (16).

$$I = 547.01e^{-(\frac{T-157.3}{81.86})^2} \tag{16}$$

C. COMBINED EFFECT OF PRESSURE AND TEMPERATURE ON PD ACTIVITY

To determine the combined impact of p_g and T on PD characteristic parameters, the moderation of experimental data was carried out. The moderation effect was investigated by introducing a third variable (p_g or T) in the relationship between two variables given in (11) to (16) [35]. The coefficients of variance (β) determined from individual and combined effect of p_g and T on PD characteristic parameters are shown in Table 1. From Table 1, it can be observed that the combined effect of p_g and T on PD characteristic parameters results in the positive significant increase in the value of β and hence, produce an enhancing moderation effect which develop a stronger relationship.

The relationships were developed for CE, q_a, and I as a function of both p_g and T using curve fitting technique. The R-square goodness of fit hypothesis was applied to measure the closeness of data with the fitted line. Based on the results of R-square goodness of fit hypothesis, the plausibility of two terms Gaussian model was established. The results of two term Gaussian model are given in (17), (18) and (19).

$$CE = 577.4e^{-(\frac{p_gT-3.244\times10^5}{1.673\times10^5})^2} + 49.14e^{-(\frac{p_gT-7.688\times10^4}{9.532\times10^4})^2} \tag{17}$$

$$I = 1.337\times10^5 e^{-(\frac{p_gT-3.664\times10^5}{1.6332\times10^5})^2} + 6141e^{-(\frac{p_gT-1.124\times10^5}{1.005\times10^5})^2} \tag{18}$$

$$q_a = 1206.19e^{-(\frac{p_gT-3.332\times10^5}{1.663\times10^5})^2} + 89.51e^{-(\frac{p_gT-8.449\times10^4}{9.612\times10^4})^2} \tag{19}$$

The physical phenomena related to the pressure and temperature have been already discussed in subsections IV.A and IV.B. Once the pressure decreases at high temperature, the PD electrons gain more thermal energy due to which there

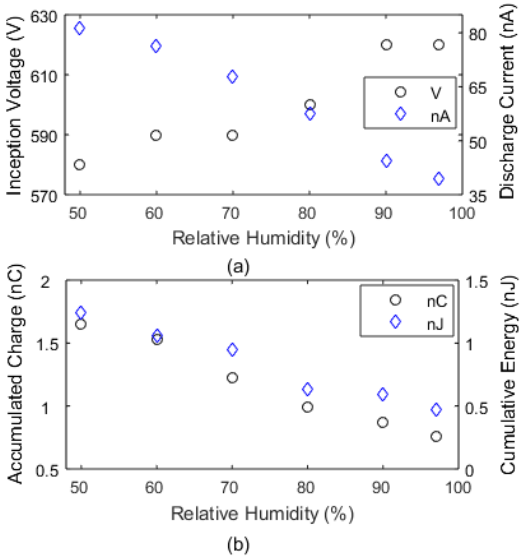

FIGURE 11. The measurement of various PD quantities for different *RH* levels at ambient pressure and 30° C temperature (a) inception voltage and discharge current, (b) accumulated charge and cumulative energy.

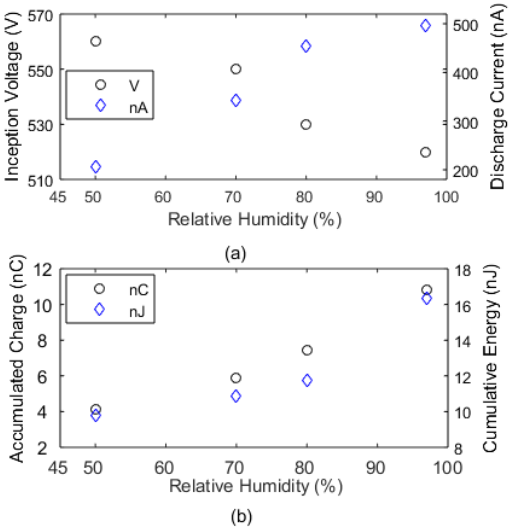

FIGURE 12. The measurement of various PD quantities for different *RH* levels at ambient pressure and 90° C temperature (a) inception voltage and discharge current, (b) accumulated charge and cumulative energy.

is a reduction in the relative air density. This results in the additional increase of electron mean free path as given in (8) and (9). Furthermore, when pressure is increased at high temperature, PD electrons gain more energy leading to less energy dissipation in thermal diffusion, and more is injected into the discharge process. Therefore, at high temperatures, increasing the relative pressure makes the discharge more harmful, accelerating the rate of the insulation degradation, resulting in a shorter lifetime [22].

D. EFFECT OF HUMIDITY ON PD ACTIVITY

The impact of variation in the humidity on PD activity was investigated at both low and high T levels (30° C and 90° C). In the first experiment, the temperature in the environmental chamber was adjusted at 30° C and the discharge characteristics of the PD signal were measured by varying the humidity inside the chamber from 50% to 97%. At low T, increase in humidity resulted in the decrease of the PD activity, as shown in Fig. 11. From Fig. 11 it is clear that the increase in *RH* from 50% to 97% caused the U_i to increase by 3.4% and I to decrease by 26%. Similarly, q_a and CE also decreased by 54% and 78% respectively.

The experiments were repeated by adjusting the T of the chamber at 90° C. This led to the different behavior of PD activity versus humidity. Consequently, the variation of *RH* from 50% to 97% at high temperatures led to an increase in the PD activity. Figure 12 shows that the variation of *RH* from 50% to 97% resulted in decrease of the U_i by 9% and increase of I by 140%. Similarly, q_a and *CE* also increased by 160% and 67% respectively.

PD activity at different humidity levels is dependent upon T. When PD occurs in the motor insulation, different byproducts are formed due to the discharges. When humidity is increased at low T, these byproducts interact with the moisture and form a semi-conductive layer on the insulation surface [36], [37]. The surface discharges are produced and the endurance of electrical insulation is enhanced when surface discharges are more prominent. Similar results have been reported in [15]. When *RH* is increased at high T, the moisture on the insulation surface decreases and no semi-conductive layer is formed due to the absence of water molecules. In this case, the internal discharges are more prominent due to low surface discharges and the endurance of insulation material is reduced.

E. EFFECT OF CONTAMINATION ON PD ACTIVITY

The effect of contamination on PD behavior in winding insulation of low voltage motor was studied. It was found that the effect of contamination depends upon the concentration and the nature of contaminants as well as humidity level. To carry out this study, the contaminated environment was developed in the climate-controlled chamber and experiments were performed at both low and high *RH* levels (30% *RH* and 90% *RH*). The contaminant was prepared using a calculated amount of salt particles and iron grains in a specific weight ratio (1:1). The mixture was sprayed on the stator winding insulation. The smoke was formed by burning the carbon [38], diluted with the air in a specific volume ratio (5:1) and further drawn through an inlet valve. The stator insulation under contamination is shown in Fig. 13.

In the first experiment, PD measurements were conducted at ambient T and 30% *RH* conditions for different contamination levels (from ambient level to 0.25 kg/m^3). The increase in the contamination level up to 0.25 kg/m^3 at low *RH* (30%) resulted in decreasing the U_i by 15%. The variations in PD characteristic parameters with the contamination at 30% *RH* are shown in Fig. 14. At low *RH* (30%), the increase in the contamination increased the PD activity and vice versa.

FIGURE 13. The view of a motor stator for PD measurement under contamination.

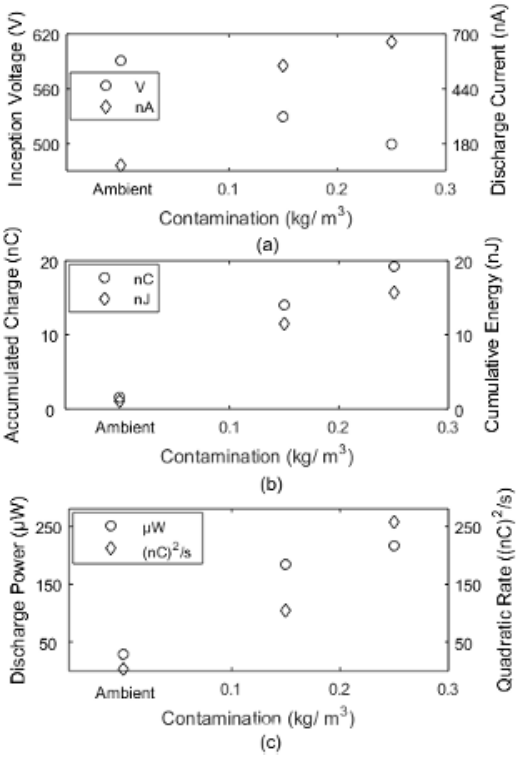

FIGURE 14. PD characteristics measured for different contamination levels at ambient temperature (35° C), pressure (1000 mbar) and 30% *RH* (a) inception voltage and average discharge current, (b) accumulated apparent charge and cumulative energy, (c) discharge power and quadratic rate.

In the second experiment, the *RH* in the climate-controlled chamber was adjusted at 90% and the concentration of contaminants was again varied from ambient level to 0.25 kg/m^3. The CE and other characteristics of the PD signals were measured. At high RH, the increase in contamination decreased the PD activity, as shown in Fig. 15. From Fig. 15, it can be observed that by changing the contamination level from ambient to 0.25 kg/m^3, U_i increased by 12%. The magnitude of I, q_a, and CE also increased by 71%, 300% and, 350% respectively.

PD measurement at different contaminant levels is a function of *RH*. When contaminants in the air are increased at high *RH* levels, they interact with the moisture and form a conductive layer on the insulation surface. The external

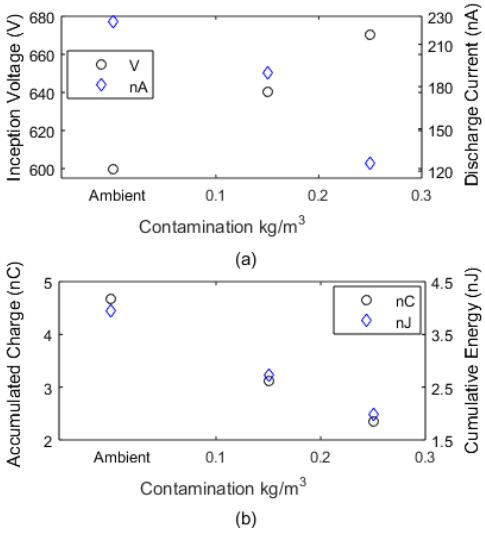

FIGURE 15. PD quantities measured for different contamination levels at 90% *RH*, ambient pressure and temperature (a) inception voltage and discharge current, (b) accumulated charge and cumulative energy.

discharges are produced and the endurance of electrical insulation is enhanced. PD activity is reduced as discussed in the subsection IV.D. When contamination was increased at low *RH*, no conductive layer is formed due to the absence of moisture on the insulation surface. In this situation, internal discharges are more prominent.

V. INSULATION LIFETIME ESTIMATION

The lifetime of stator insulation in low voltage induction motor was estimated as a function of average discharge current (I) under different environmental stresses. For this purpose, two out of four motors from different manufacturers were selected to carry out the aging tests under PD at ambient environmental conditions. The test voltage ($1.5 \times U_i$) was applied and I was measured. The magnitude of I in both motors increased with time. The constant test voltage was applied until the breakdown of both motors occurred. The magnitude of I in both motors was measured at the time of breakdown. The magnitude of I was taken as a reference value and the remaining two motors were tested at different pressures, temperatures, humidity, and contamination. The test voltage ($1.5 \times U_i$) was applied under the specific environmental conditions and similar to the previous situation, I increased with time. When the magnitude of I increased to such a value that it approaches the reference value measured at the ambient conditions, the time of the applied test voltage on stator insulation was recorded. The calculated time is the estimated insulation lifetime of the low voltage motor. The test was repeated using both motors under different environmental stresses and the impact of these stresses on the insulation lifetime was determined.

A. EFFECT OF PRESSURE ON THE INSULATION LIFETIME

Aging tests were performed in the pressure range from 180 mbar to 1750 mbar at ambient T and humidity

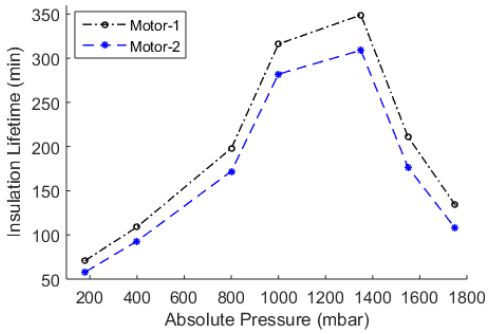

FIGURE 16. Estimated insulation lifetime as a function of absolute pressure at $U = 1.5 \times U_i$, $I = 832$ nA, ambient temperature and humidity.

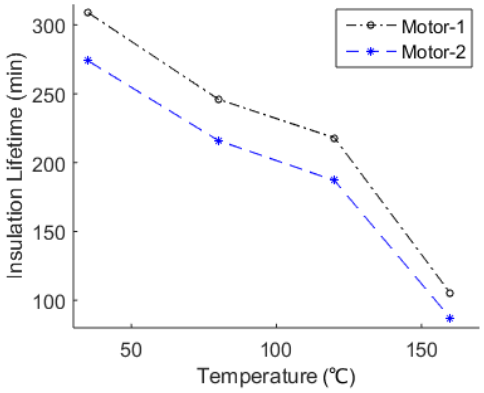

FIGURE 17. Estimated insulation lifetime as a function of temperature at $U = 1.5 \times U_i$, $I = 832$ nA, ambient pressure and ambient humidity.

levels. Fig. 16 shows the variation of the lifetime of insulation of two motors as a function of positive and negative p at $1.5 \times U_i$. With the increase in p from 180 mbar to 1350 mbar, the lifetime of the insulation increased by 390-430%. The lifetime of the insulation reduced by 62-65% upon further increasing the p from 1350 mbar to 1750 mbar.

B. EFFECT OF TEMPERATURE ON THE INSULATION LIFETIME

The insulation lifetime was estimated as a function of T at atmospheric p and humidity, by applying $1.5 \times U_i$. The variation of the lifetime of insulation of two motors with T is shown in Fig. 17. From Fig. 17, it can be observed from this figure that the insulation lifetime reduced by 66-68% upon increasing T from 35° C to 160° C. Hence, the increase in T decreases the lifetime of the winding insulation and thus, can be considered as a threat to the life expectancy of the motor.

C. EFFECT OF HUMIDITY ON THE INSULATION LIFETIME

The insulation lifetime was estimated at various humidity levels at two different T by applying $1.5 \times U_i$. The variation in the lifetime estimation of the insulation of two motors with humidity at 30° C and 90° C is shown in Fig. 18. At 30° C, the insulation lifetime increased by 33-36% upon increasing the RH from 50% to 97%. The lifetime of the insulation reduced

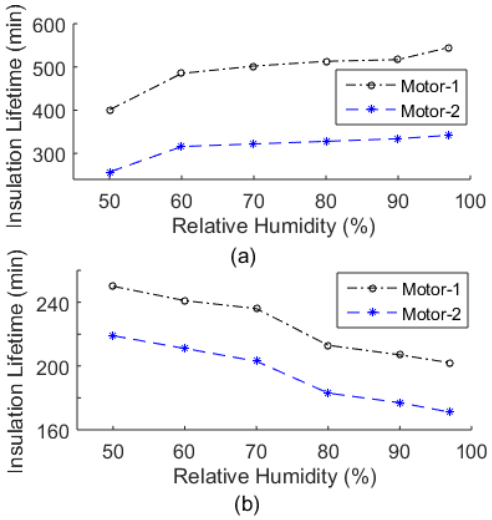

FIGURE 18. Estimated insulation lifetime as a function of humidity at two different temperatures (a) 30° C and (b) 90° C at $U = 1.5 \times U_i$ and ambient pressure.

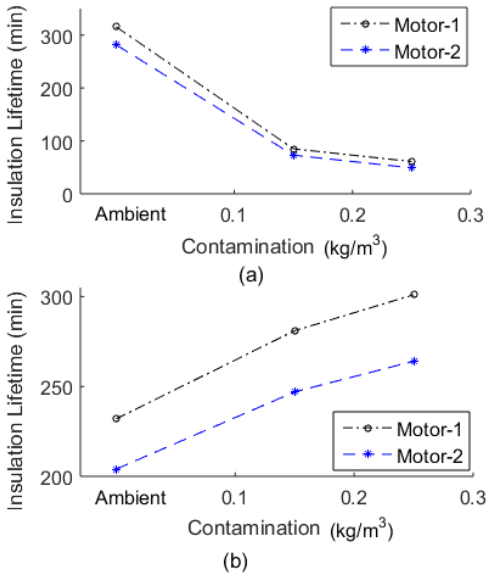

FIGURE 19. Estimated insulation lifetime as a function of contamination at two different humidity levels (a) 30% RH and (b) 90% RH at $U = 1.5 \times U_i$, ambient temperature, and pressure.

by 19-22% at 90° C upon increasing the RH from 50% to 97%. Therefore, the exact estimation of insulation lifetime with humidity is possible only if the atmospheric T is also taken into consideration.

D. EFFECT OF CONTAMINATION ON THE INSULATION LIFETIME

The insulation lifetime was estimated as a function of contamination at two different RH levels by applying $1.5 \times U_i$. Fig. 19 shows the variation in the lifetime of the insulation of the two motors with contamination at 30% RH and 90% RH. At 30% RH, the insulation lifetime reduced by 80-83% upon increasing the contamination level up to 0.25 kg/m^3. The

lifetime of the insulation increased by 28-30% at 90% *RH* by increasing the contamination up to 0.25 kg/m^3. Therefore, it is important to consider the *RH* level for the estimation of insulation lifetime with the contamination.

VI. CONCLUSION

The combined effect of electrical and environmental stresses on motor insulation is the escalation of the insulation degradation and reduces its lifetime. Various PD characteristic parameters including PD inception voltage U_i, accumulated charge q_a, cumulative energy CE, average discharge current I, discharge power P, and quadratic rate D were studied under different environmental conditions including various levels of pressure p, temperature T, relative humidity RH, and contamination on motor insulation, tested in a climate-controlled chamber.

It was observed that an increase in p from 180 mbar to 1350 mbar resulted in increase of the insulation lifetime by 390-430%. The insulation lifetime decreased by 62-65% upon further increasing the p from 1350 mbar to 1750 mbar. The severity of PD at high negative p level is more than the severity at high positive p. Furthermore, the results show that the increase in temperature increases the PD characteristics. Therefore, the insulation lifetime reduced by 66-68% upon increasing T from 35° C to 160° C. The PD activity indicated that an increase in temperature resulted in high PD magnitude but lower number of PD pulses. Only weaker points in insulation are significantly affected by the variation in the temperature. The effect of humidity on the PD characteristic and the insulation lifetime depends upon the temperature. At high temperature ($T = 90°$ C), the lifetime of the insulation reduced by 19-22% upon increasing the *RH* from 50% to 97%. However, at low temperature ($T = 30°$ C), the PD activity decreased and the insulation lifetime increased by 33-36% upon increasing the humidity level from 50% to 97%. This is mainly attributed to the interaction of the discharge byproducts and the water molecules, resulting in formation of a conductive layer at the surface of the insulation. The same conductive layer is formed due to the interaction of the contaminants with the water molecule at a high humidity level. Consequently, the PD activity decreased and the lifetime of the insulation increased. The experimental results of the humidity at low temperature and the contamination at high humidity suggest that the endurance of insulation can be improved by increasing the surface conductivity.

REFERENCES

[1] G. C. Stone, H. G. Sedding, and C. Chan, "Experience with online partial-discharge measurement in high-voltage inverter-fed motors," *IEEE Trans. Ind. Appl.*, vol. 54, no. 1, pp. 866–872, Jan. 2018.

[2] A. Hughes and B. Drury, *Electric Motors and Drives: Fundamentals, Types and Applications*, 4th ed. Boston, MA, USA: Elsevier & Newnes, 2013.

[3] *Rotating Electrical Machines—Part 25: AC Electrical Machines Used in Power Drive Systems—Application Guide*, Standard IEC TS 60034-25:2014, 2014.

[4] P. Bidan, T. Lebey, and C. Neacsu, "Development of a new off-line test procedure for low voltage rotating machines fed by adjustable speed drives (ASD)," *IEEE Trans. Dielectr. Electr. Insul.*, vol. 10, no. 1, pp. 168–175, Feb. 2003.

[5] A. Mbaye, F. Grigorescu, T. Lebey, and B. Ai, "Existence of partial discharges in low-voltage induction machines supplied by PWM drives," *IEEE Trans. Dielectr. Electr. Insul.*, vol. 3, no. 4, pp. 554–560, Aug. 1996.

[6] O. M. Nassar, "Motor insulation degradation due to switching surges and surge protection requirements," *IEEE Trans. Energy Convers.*, vol. EC-1, no. 3, pp. 182–189, Sep. 1986.

[7] A. H. Bonnett, "Analysis of the impact of pulse-width modulated inverter voltage waveforms on AC induction motors," *IEEE Trans. Ind. Appl.*, vol. 32, no. 2, pp. 386–392, Mar./Apr. 1996, doi: 10.1109/28.491488.

[8] M. Kurtz, J. F. Lyles, and G. C. Stone, "Application of partial discharge testing to hydro generator maintenance," *IEEE Trans. Power App. Syst.*, vol. PAS-103, no. 8, pp. 2148–2157, Aug. 1984.

[9] P. Morshuis, "Assessment of dielectric degradation by ultrawide-band PD detection," *IEEE Trans. Dielectr. Electr. Insul.*, vol. 2, no. 5, pp. 744–760, Oct. 1995.

[10] G. C. Stone and V. Warren, "Effect of manufacturer, winding age and insulation type on stator winding partial discharge levels," *IEEE Elect. Insul. Mag.*, vol. 20, no. 5, pp. 13–17, Sep. 2004.

[11] A. B. J. M. Driessen, J. van Duivenbode, and P. A. A. F. Wouters, "Operational conditions influencing the partial discharge performance of cables under low and medium vacuum," *IEEE Trans. Dielectr. Electr. Insul.*, vol. 26, no. 1, pp. 81–89, Feb. 2019.

[12] L. A. Dissado and J. C. Fothergill, *Electrical Degradation and Breakdown in Polymers*, vol. 9. Edison, NJ, USA: IET, 1992.

[13] A. Küchler, *High Voltage Engineering: Fundamentals-Technology-Applications*. Berlin, Germany: Springer-Verlag, 2017.

[14] K. Younsi, D. Snopek, J. Hayward, P. Menard, and J. C. Pellerin, "Seasonal changes in partial discharge activity on hydraulic generators," in *Proc. Electr. Insul. Conf. Electr. Manuf. Coil Winding Conf.*, Oct. 2001, pp. 423–428.

[15] M. Fenger and G. C. Stone, "Investigations into the effect of humidity on stator winding partial discharges," *IEEE Trans. Dielectr. Electr. Insul.*, vol. 12, no. 2, pp. 341–346, Apr. 2005.

[16] L. Lin, A. Kang, J. Song, Z. Lei, Y. Zhao, and C. Feng, "Influences of humidity and temperature on oil contamination discharge of HV motor stator windings," *IEEE Trans. Dielectr. Electr. Insul.*, vol. 23, no. 5, pp. 2695–2703, Oct. 2016.

[17] C. Emersic, R. Lowndes, I. Cotton, S. Rowland, and R. Freer, "The effects of pressure and temperature on partial discharge degradation of silicone conformai coatings," *IEEE Trans. Dielectr. Electr. Insul.*, vol. 24, no. 5, pp. 2986–2994, Oct. 2017.

[18] J. V. Champion, S. J. Dodd, A. S. Vaughan, Y. Zhao, and S. J. Sutton, "The effect of voltage, temperature and morphology on electrical treeing in polyethylene blends," in *Proc. 8th Int. Conf. Dielectr. Mater., Meas. Appl.*, Edinburgh, U.K., 2000, pp. 35–40, doi: 10.1049/cp:20000473.

[19] R. Schifani, R. Candela, and P. Romano, "On PD mechanisms at high temperature in voids included in an epoxy resin," *IEEE Trans. Dielectr. Electr. Insul.*, vol. 8, no. 4, pp. 589–597, Aug. 2001.

[20] T. Dakin and C. Works, "Measurement of corona discharge behavior at low pressure and vacuum," in *Measurement of Dielectric Properties Under Space Conditions*. West Conshohocken, PA, USA: ASTM International, 1967.

[21] R. Rui and I. Cotton, "Impact of low pressure aerospace environment on machine winding insulation," in *Proc. IEEE Int. Symp. Electr. Insul.*, Jun. 2010, pp. 1–5.

[22] E. Sili, J. P. Cambronne, N. Naude, and R. Khazaka, "Polyimide lifetime under partial discharge aging: Effects of temperature, pressure and humidity," *IEEE Trans. Dielectr. Electr. Insul.*, vol. 20, no. 2, pp. 435–442, Apr. 2013.

[23] *High-Voltage Test Techniques—Partial Discharge Measurements*, International Standard IEC-60270, 2000.

[24] J. H. Dymond, N. Stranges, K. Younsi, and J. E. Hayward, "Stator winding failures: Contamination, surface discharge, tracking," *IEEE Trans. Ind. Appl.*, vol. 38, no. 2, pp. 577–583, Mar./Apr. 2002.

[25] G. M. Hashmi, *Partial Discharge Detection for Condition Monitoring of Covered-Conductor Overhead Distribution Networks Using Rogowski Coil*. Espoo, Finland: Teknillinen korkeakoulu, 2008.

[26] G. A. Hussain, "Methods for arc-flash prediction in medium voltage and low voltage switchgear," Ph.D. dissertation, Aalto Univ., Espoo, Finland, 2015.

[27] J. Kuffel and P. Kuffel, *High Voltage Engineering Fundamentals*. Amsterdam, The Netherlands: Elsevier, 2000.

[28] M. Shafiq, "Design and implementation of partial discharge measurement sensors for on-line condition assessment of power distribution system components," Ph.D. dissertation, Aalto Univ., Espoo, Finland, 2015.
[29] *Rotating Electrical Machines—Part 27-1: Off-Line Partial Discharge Measurements on the Winding Insulation*, Standard IEC 60034-27, 2006.
[30] G. A. Hussain, L. Kumpulainen, J. V. Kluss, M. Lehtonen, and J. A. Kay, "The smart solution for the prediction of slowly developing electrical faults in MV switchgear using partial discharge measurements," *IEEE Trans. Power Del.*, vol. 28, no. 4, pp. 2309–2316, Oct. 2013.
[31] H. H. Sinaga, B. T. Phung, and T. R. Blackburn, "Partial discharge localization in transformers using UHF detection method," *IEEE Trans. Dielectr. Electr. Insul.*, vol. 19, no. 6, pp. 1891–1900, Dec. 2012.
[32] M. D. Judd, L. Yang, and I. B. B. Hunter, "Partial discharge monitoring of power transformers using UHF sensors. Part I: Sensors and signal interpretation," *IEEE Elect. Insul. Mag.*, vol. 21, no. 2, pp. 5–14, Mar. 2005.
[33] I. Rtca, "Environmental conditions and test procedures for airborne equipment," RTCA, Inc, Tech. Rep., 2007.
[34] P. Tardiveau, E. Marode, A. Agneray, and M. Cheaib, "Pressure effects on the development of an electric discharge in non-uniform fields," *J. Phys. D, Appl. Phys.*, vol. 34, no. 11, p. 1690, 2001.
[35] J. Cohen, P. Cohen, S. G. West, and L. S. Aiken, *Applied Multiple Regression/Correlation Analysis for the Behavioral Sciences*. Evanston, IL, USA: Routledge, 2013.
[36] C. Hudon, R. Bartnikas, and M. R. Wertheimer, "Surface conductivity of epoxy specimens subjected to partial discharges," in *Proc. IEEE Int. Symp. Electr. Insul.*, Jun. 1990, pp. 153–155.
[37] P. Morshuis and F. Kreuger, "Transition from streamer to townsend mechanisms in dielectric voids," *J. Phys. D: Appl. Phys.*, vol. 23, no. 12, p. 1562, 1990.
[38] P. J. DiNenno, *SFPE Handbook of Fire Protection Engineering*. New York, NY, USA: Springer-Verlag, 2008.

WAQAR HASSAN received the B.Sc. and M.Sc. degrees in electrical engineering from the University of Engineering and Technology Lahore (UET), Lahore, Pakistan, in 2010 and 2014, respectively, and the M.B.A. degree (Executive) from the University of Sargodha, Sargodha, Pakistan, in 2016. He is currently pursuing the Ph.D. degree in electrical engineering with UET Lahore. He has nine years of experience in installation, testing and commissioning of MV substations, electric power plants, and HVAC chillers. He was a Lecturer with the Electrical Engineering Department, The University of Lahore, Lahore, and the Noon Business School, University of Sargodha. His research interests include partial discharges in power systems, power system quality, and electric grounding systems.

GHULAM AMJAD HUSSAIN (Senior Member, IEEE) received the bachelor's degree in electrical engineering from the University of Engineering and Technology Lahore, Lahore, Pakistan, in 2007, and the master's and Ph.D. degrees from the School of Electrical Engineering, Aalto University, Finland, in 2012 and 2016, respectively. He was a Senior Research and Development Engineer in power systems technologies with the EATON European Innovation Centre (EEIC), Prague, Czech Republic. He is currently an Assistant Professor with the American University of Kuwait, Kuwait, where he is involved in teaching and research. He has authored/coauthored more than 40 articles in international journals and conferences. He holds one patent. His research interests include high-voltage engineering, power system protection, control in modern smart grids, and power system analysis.

FARHAN MAHMOOD received the B.Sc. and M.Sc. degrees in electrical engineering from the University of Engineering and Technology (UET) Lahore, Lahore, Pakistan, in 2005 and 2007, respectively, and the Ph.D. degree from Aalto University, Espoo, Finland, in 2016. He is currently an Assistant Professor with the Department of Electrical Engineering, UET Lahore. His research interests include power system transients, investigation of lightning over voltages in power systems, overvoltage protection, and insulation coordination.

SALMAN AMIN received the Ph.D. degree, in 2013. He is currently an Associate Professor with the Electrical Engineering Department, University of Engineering and Technology Taxila, Taxila, Pakistan. His research interests include power systems, high-voltage polymeric insulation, life estimation of insulation, thermoplastic materials, energy systems, composite materials, and self-healing materials.

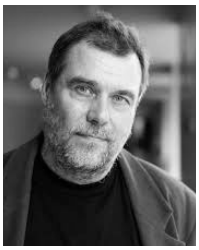

MATTI LEHTONEN (Member, IEEE) received the M.Sc. and Licentiate degrees in electrical engineering from the School of Electrical Engineering, Aalto University (Helsinki University of Technology), Espoo, Finland, in 1984 and 1989, respectively, and the D.Sc. degree from the Tampere University of Technology, Tampere, Finland, in 1992. Since 1987, he has been with VTT Energy, Espoo. Since 1999, he has been with the School of Electrical Engineering, Aalto University, where he is currently the Head of the Power Systems and High Voltage Engineering Department. His main research interests include earth fault analysis and harmonic related issues and applications of information technology in distribution automation and distribution energy management.